



Overexpression of ring finger protein 20 inhibits the progression of liver fibrosis via mediation of histone H2B lysine 120 ubiquitination

Shanshan Chen^{1,2} · Xuan Dai^{1,3} · Hong Li^{1,4} · Yuhuan Gong^{1,4} · Yueyue Zhao^{1,2} · Haijun Huang¹

Received: 16 September 2020 / Accepted: 25 January 2021
© Japan Human Cell Society 2021

Abstract

Liver fibrosis is a chronic liver injury that leads to liver cirrhosis and liver cancer. Ring finger protein 20 (RNF20), also named as E3 ubiquitin-protein ligase BRE1A, has been reported to be involved in chronic liver diseases. However, the role of RNF20 in liver fibrosis remains unclear. To mimic liver fibrosis in vitro, LX-2 cells were treated with TGF-β. Gene and protein expressions were detected by RT-qPCR and western blot, respectively. The mechanism by which RNF20 mediated the progression of liver fibrosis was explored by bioinformatics analysis. Finally, *in vivo* mouse model of liver fibrosis was established to detect the function of RNF20. The results indicated that TGF-β-induced increase of cell viability and migration was significantly reversed by RNF20 overexpression. Consistently, overexpression of RNF20 significantly reversed TGF-β-induced activation of fibrotic proteins in LX-2 cells. Meanwhile, VEGFA, TNF-α and IL-6 were found to be the downstream targets of RNF20 in LX-2 cells. Moreover, RNF20 overexpression notably inhibited the progression of liver fibrosis via ubiquitination of H2B. Finally, RNF20 upregulation significantly attenuated the symptom of liver fibrosis *in vivo*. In summary, overexpression of RNF20 significantly inhibited the progression of liver fibrosis *in vitro* and *in vivo*. Therefore, RNF20 might serve as a new target for the treatment of liver fibrosis.

Keywords Liver fibrosis · RNF20 · H2BK120ub · Ubiquitination

Introduction

Liver fibrosis is considered as the outcomes after repairs of liver injury [1]. It is manifested by excessive deposition of extracellular matrix components in the liver, which can further develop into irreversible and highly lethal liver diseases such as cirrhosis or hepatocellular carcinoma (HCC)

[2, 3]. Nowadays, the major treatment of liver fibrosis is drug therapy [4], while the effect is still limited. Thus, it is essential to find new strategies for the treatment of liver fibrosis.

Ring finger protein 20 (RNF20), an ortholog of yeast Bre1A, is an E3 ligase that ubiquitinates histone H2B 120 lysine [5]. RNF20 is known to be participated in many biological events, such as cell division and transcription [6, 7]. Particularly, aberrant expression of RNF20 leads to ectopic lipid accumulation in the liver [8], which can mediate the progression of chronic liver diseases. However, the role of RNF20 in liver fibrosis remains unclear.

RNF20 and H2B monoubiquitination (H2Bub) have been shown to be important for a variety of biological processes, such as DNA replication [9], gene transcription [10], and tumorigenesis [11]. Meanwhile, ubiquitylation of histone H2B at lysine residue 120 (H2BK120ub) is a prominent histone posttranslational modification (PTM) which is localized primarily to actively transcribed genes [12]. Furthermore, H2BK120ub mark has also been implicated in the DNA damage response (DDR) to double-strand breaks where it is thought to have a role in decompacting chromatin structure during the repairs of tissue injury [13]. A previous report

Shanshan Chen, Xuan Dai contributed equally to this study.

✉ Haijun Huang
huanghaijun0826@163.com

¹ Department of Infectious Disease, Zhejiang Provincial People's Hospital and People's Hospital Affiliated of Hangzhou Medical College, No. 158 Shangtang Road, Hangzhou 310014, Zhejiang, China

² Graduate School of Clinical Medicine, Bengbu Medical College, Bengbu 233000, Anhui, China

³ Zhejiang Academy of Medical Sciences, Hangzhou 310013, Zhejiang, China

⁴ Medical College of Qingdao University, Qingdao 266071, Shandong, China

has indicated a functional crosstalk between RNF20 and H2BK120ub [14]. However, the correlation between RNF20 and H2BK120ub in liver fibrosis remains unclear.

In the current study, we aimed to investigate the role of RNF20 in liver fibrosis. We hope the current study would shed new lights on exploring the treatment of liver fibrosis.

Material and methods

Tissue collection

Ten tissues of S1-2 phase (chronic hepatitis B, CHB) and ten tissues of S3-4 phase liver fibrosis tissues (Hepatitis B Cirrhosis, HBC) were collected from Zhejiang Provincial People's Hospital between August 2019 and May 2020. Clinical and pathological data of these patients were collected with their written informed consent. This research was approved by the Institutional Ethical Committee of Zhejiang Provincial People's Hospital. The clinical information of patients was listed in Table 1. Meanwhile, ten S1-2 phase tissues and ten S3-4 phase tissues of patients with liver fibrosis were used for investigating the protein levels of H2B, H2BK120ub and RNF20 (Table 1). In addition, five

S1-2 phase tissues and five S3-4 phase tissues of patients with liver fibrosis were used for investigating the level of PPAR γ . The stage of liver fibrosis was classified according to the previous reference [15]. The clinical information was presented in Table 1.

Cell culture and treatment

Human hepatic stellate cell lines (LX-2) were obtained from the Institute of Biochemistry and Cell Biology of the Chinese Academy of Sciences (Shanghai, China). The 293 T cells were obtained from the American Type Culture Collection (ATCC, Manassas, VA, USA). Cells were cultured in RPMI-1640 medium (Gibco, Carlsbad, CA, USA) supplemented with 10% fetal bovine serum (Gibco) and penicillin (100 U/mL). In addition, cells were cultured in the condition of 37 °C and 5% CO₂. To mimic liver fibrosis in vitro, LX-2 cells were treated with 5 ng/ml TGF- β for 24 h.

Bioinformatics analysis

Differentially expressed genes among LX-2 cells, TGF- β -treated LX-2 cells and TGF- β +RNF20-treated LX-2 cells were obtained from RNA-seq as previously described [16]. Volcano plots and heat map were performed to assess the differentially expressed genes among LX-2 cells, TGF- β -treated LX-2 cells and TGF- β +RNF20-treated LX-2 cells. GO analysis was performed to explore the functions of genes in terms of biological processes, cellular components and molecular functions. Biological pathways were assessed in the Kyoto Encyclopedia of Genes and Genomes (KEGG).

Cell transfection

For in vitro study, LX-2 cells were transfected with pcDNA3.1, pcDNA3.1-RNF20, pcDNA3.1-H2BK120R or pcDNA3.1-H2BWT using Lipofectamine 2000. pcDNA3.1, pcDNA3.1-RNF20, pcDNA3.1-H2BK120R and pcDNA3.1-H2BWT were obtained from Hanbio (Shanghai, China). Plasmids expressing H2BWT and H2BK120R were constructed by cloning wild-type or lysine 120 to arginine mutated H2B PCR products into the pcDNA3.1 vectors. LX-2 cells were transfected with H2BK120R OE or H2BWT OE using Lipofectamine 2000. The efficiency of cell transfection was investigated by RT-qPCR.

Adeno-associated virus infection

In animal study, adeno-associated virus (AAV) was used for RNF20 overexpression. The pAV-TBG-RNF20 (AAV8-RNF20) was synthesized by Vigene (Jinan, China). 293 T cells were transfected with pAV-TBG-RNF20 (AAV8-RNF20). After 24 h of transfection, the supernatants

Table 1 The clinical information of patients

Patient (No.)	Age	Sex	Liver fibrosis stage*	Hepatitis grade
1	35	Male	S1	G1
2	40	Male	S1	G1-2
3	38	Male	S1	G1
4	50	Male	S1	G1
5	44	Male	S1	G2
6	48	Male	S2	G1
7	24	Male	S2	G2
8	26	Male	S2	G2
9	49	Female	S2	G2
10	36	Female	S2	G1-2
11	49	Male	S3	G2
12	40	Male	S3	G2
13	49	Female	S3	G2
14	50	Male	S3	G2
15	36	Male	S3	G1
16	41	Female	S4	G2
17	42	Male	S4	G3
18	44	Female	S4	G2
19	47	Male	S4	G2
20	42	Male	S4	G1

G grade, S stage

*The stage of hepatitis was in accordance with the previous reference: [15]

containing virus particles of AAV-RNF20 were collected and filtered [16]. The viral titer of AAV8-RNF20 was 7.94×10^{13} vg/ml. Meanwhile, the information of plasmids and AAV8 virus was provided in supplementary material.

Quantitative real time polymerase chain reaction (RT-qPCR)

Total RNA was extracted from LX-2 cells or liver tissues using TRIzol reagent (TaKaRa, Tokyo, Japan) according to the manufacturer's protocol. cDNA was synthesized using the reverse transcription kit (TaKaRa, Ver.3.0) according to the manufacturer's protocol. Real-Time qPCRs were performed in triplicate under the following protocol: 10 min at 95 °C, followed by 35 cycles of 15 s at 95 °C and 1 min at 60 °C. The primers were obtained from GenePharma (Shanghai, China). RNF20: forward, 5'-TGA GAAGTCAGGTGTGCGTA-3' and reverse 5'-AGAGAC TTCTTCCAGGCAAC-3'. IL-6: forward, 5'-AGACAG CCACTCACCTCTTCA-3' and reverse 5'-CACCAAGGCA AGTCTCCTCAT-3'. VEGFA: forward, 5'-TGCTCTTACC TCCACCATGC-3' and reverse 5'-AGGTTTGATCCGCAT AATCTG-3'. TNF- α : forward, 5'-CTCTTCTCCTTCCTG ATCGTG-3' and reverse 5'-TTTGCTACAACATGGGCT ACA-3'. GAPDH: forward, 5'-GCCTTCCGTGTCCCC ACTGC-3' and reverse 5'-GGCTGGTGGTCCAGGGGT CT-3'. $2^{-\Delta\Delta Ct}$ method was used to quantify the results, and GAPDH was used for normalization.

CCK-8 assay

LX-2 cells were seeded in 96-well plates (5×10^3 per well) overnight. Then, cells were treated with TGF- β , TGF- β + vector, TGF- β + RNF20 overexpression (OE), TGF- β + H2BK120R OE or TGF- β + H2BWT OE for 72 h. 10 μ l CCK-8 reagents were added to each well and cells were incubated for 2 h at 37 °C. Finally, the absorbance of LX-2 cells was measured at 450 nm using a microplate reader (Thermo Fisher Scientific).

Wound healing assay

LX-2 cells were plated into a 24-well Cell Culture Cluster and allowed to grow to 80–90% confluence. Then, cells were underlined perpendicular to the cell culture plate with a small pipette head. After washing with PBS three times, serum-free medium was used for further culture, and the scratch widths at 0 and 24 h were recorded under an optical microscope.

Western blot detection

Total protein was isolated from cell lysates or tissues using RIPA buffer. The concentration of protein was detected with a BCA protein kit (Thermo Fisher Scientific). Then, proteins (40 μ g per lane) were separated with 10% SDS-PAGE gel and then transferred into polyvinylidene fluoride (PVDF, Thermo Fisher Scientific) membranes. After blocking with 3% skim milk for 1 h, the membranes were incubated with primary antibodies at 4 °C overnight. Subsequently, membranes were incubated with secondary anti-rabbit antibody (Abcam; 1:5000) at room temperature for 1 h. Membranes were scanned using an Odyssey Imaging System and analyzed with Odyssey v2.0 software (LICOR Biosciences, Lincoln, NE, USA). The primary antibodies used in this study were as follows: anti-collagen I (Abcam, Cambridge, MA, USA; 1:1000), anti-RNF20 (Abcam; 1:1000), anti-H2BK120ub (Abcam; 1:1000), anti-PPAR γ (Abcam; 1:1000), anti-H2B (Abcam; 1:1000), anti- α -SMA (Abcam; 1:1000) and anti-GAPDH (Abcam; 1:1000). GAPDH was used as an internal control.

In vivo model of liver fibrosis

C57BL/6 J mice were obtained from the Chinese Academy of Sciences (Shanghai, China). CCl4 was also dissolved in olive oil at a proportion of 1:10. Mice were randomly divided into five groups: (1) control, (2) CCl4 (2 weeks), (3) CCl4 (4 weeks), (4) CCl4 (8 weeks) and (5) CCl4 + AAV-RNF20. CCl4 (0.5 mg/kg) was intraperitoneally injected into the mice twice a week for 2, 4 or 8 weeks. Meanwhile, AAV-RNF20 virus (1×10^9 pfu/mouse) was injected through the tail vein at 2 days before the first CCl4 administration. At the end of the study, mice were sacrificed for the collection of liver tissues. Moreover, the liver tissues of mice were dissected and then symptom of liver fibrosis was detected by hematoxylin–eosin (HE) and Masson's trichrome as previously described [17, 18].

All the protocols were performed according to the guidelines of the Use Committee of Zhejiang Provincial People's Hospital (No. 20200004), and all the animal experiments were performed in accordance with National Institutes of Health guide for the care and use of laboratory animals.

Immunohistochemical (IHC) staining

Tissues of mice or patients were fixed in 4% paraformaldehyde in PBS overnight, paraffin-embedded, and cut into 5- μ m-thick sections. Paraffin sections were deparaffinized and rehydrated. The sections were heated in sodium citrate buffer in a microwave for antigen retrieval, washed with phosphate-buffered saline (PBS) for 5 min (three times) at

room temperature, incubated in 3% H₂O₂ at room temperature for 25 min, washed with PBS for 5 min (three times) and blocked and incubated in goat serum for 30 min. Then, the samples were stained with primary antibodies (anti-H2BK120ub and anti- α -SMA) overnight at 4 °C. After that, samples were incubated with secondary antibody (HRP-labeled) for 30 min at 37 °C. Finally, freshly prepared diaminobenzidine (DAB) was added for colour development. All the antibodies were obtained from Abcam. The positive hepatic stellate cells were observed under a fluorescence microscope.

Statistical analysis

Each group was performed three independent experiments and all data were expressed as the mean \pm standard deviation (SD). Differences were analyzed using Student's t-test (only two groups) or one-way analysis of variance (ANOVA) followed by Tukey's test (more than 2 groups, Graphpad Prism7). Meanwhile, the statistical analysis of age/sex correlation was performed using Chi-square test. $P < 0.05$ was considered to indicate a statistically significant difference.

Results

RNF20 and H2BK120ub were downregulated in liver fibrosis

To detect the expressions of RNF20 and H2BK120ub in patient with liver fibrosis, western blot was used. As indicated in Fig. 1a–f, the levels of RNF20, H2BK120ub and PPAR γ in S3-4 phase liver fibrosis tissues (HBC) were significantly downregulated, compared to that in S1-2 phase liver fibrosis tissues (CHB). Meanwhile, RNF20 and H2BK120ub expressions were negatively correlated with hepatitis stage of patients with liver fibrosis, while RNF20 and H2BK120ub expression were not correlated with age or sex (Fig. 1a, b; Table 2). In summary, these data revealed that RNF20, H2BK120ub and PPAR γ were downregulated in liver fibrosis.

In vitro model of liver fibrosis was successfully established

To mimic in vitro model of liver fibrosis, LX-2 cells were treated with TGF- β . As revealed in Fig. 2a, TGF- β significantly increased the viability of LX-2 cells. Moreover, migration of LX-2 cells was notably enhanced by TGF- β (Fig. 2b). In addition, protein expression of collagen I and α -SMA in LX-2 cells were significantly increased by TGF- β (Fig. 2c). In contrast, TGF- β obviously downregulated

the expressions of RNF20 and H2BK120ub in LX-2 cells (Fig. 2d). Taken together, in vitro model of liver fibrosis was successfully established.

Overexpression of RNF20 significantly inhibited TGF- β -induced fibrosis in LX-2 cells via mediation of H2BK120ub

To investigate the function of RNF20 in liver fibrosis, LX-2 cells were transfected with pcDNA3.1-RNF20, and then RT-qPCR was performed. The data indicated that the expression of RNF20 in LX-2 cells was significantly upregulated by RNF20 OE (Fig. 3a). In addition, TGF- β notably enhanced the viability of LX-2 cells, while this phenomenon was partially reversed in the presence of pcDNA3.1-RNF20 (Fig. 3b). Consistently, TGF- β -induced increase of cell migration was significantly inhibited by RNF20 overexpression (Fig. 3c). Moreover, the protein expressions of α -SMA and collagen I in LX-2 cells were notably increased by TGF- β , while the effect of TGF- β on these two proteins was reversed by pcDNA3.1-RNF20 (Fig. 3d). In contrast, TGF- β -induced inactivation of H2BK120ub and RNF20 in LX-2 cells was notably reversed by RNF20 overexpression (Fig. 3d). Altogether, overexpression of RNF20 significantly inhibited TGF- β -induced fibrosis in LX-2 cells via mediation of H2BK120ub.

Expression profiles of genes associated with RNF20-mediated liver fibrosis

To analyze the differentially expressed genes in RNF20-mediated liver fibrosis, a bioinformatics analysis of LX-2, TGF- β -treated LX-2 cells and RNF20 and TGF- β co-treated LX-2 cells was performed. The data were presented using cluster analysis and a volcano plot (Fig. 4a and b). Among the differentially expressed genes, 386 were upregulated and 139 were downregulated by TGF- β , compared with control (Fig. 4c). On the other hand, 4237 genes were upregulated and 2937 were downregulated by RNF20, compared with TGF- β alone (Fig. 4c). The overlapped differentially expressed genes among LX-2 cells, TGF- β -treated LX-2 cells and RNF20 and TGF- β co-treated LX-2 cells were presented in Fig. 5a–c.

Next, Gene Ontology (GO) and pathway analyses were performed. As shown in Fig. 5d, the most common biological process among the overlapped genes was positive regulation of cell population proliferation, cytokine-mediated signaling pathway and negative regulation of apoptotic process. Pathway analysis revealed that the overlapped genes were associated with the mitogen-activated protein kinase (MAPK), TNF and NF- κ B pathways (Fig. 5d). Meanwhile, among these three signaling pathways, TNF- α , IL-6 and

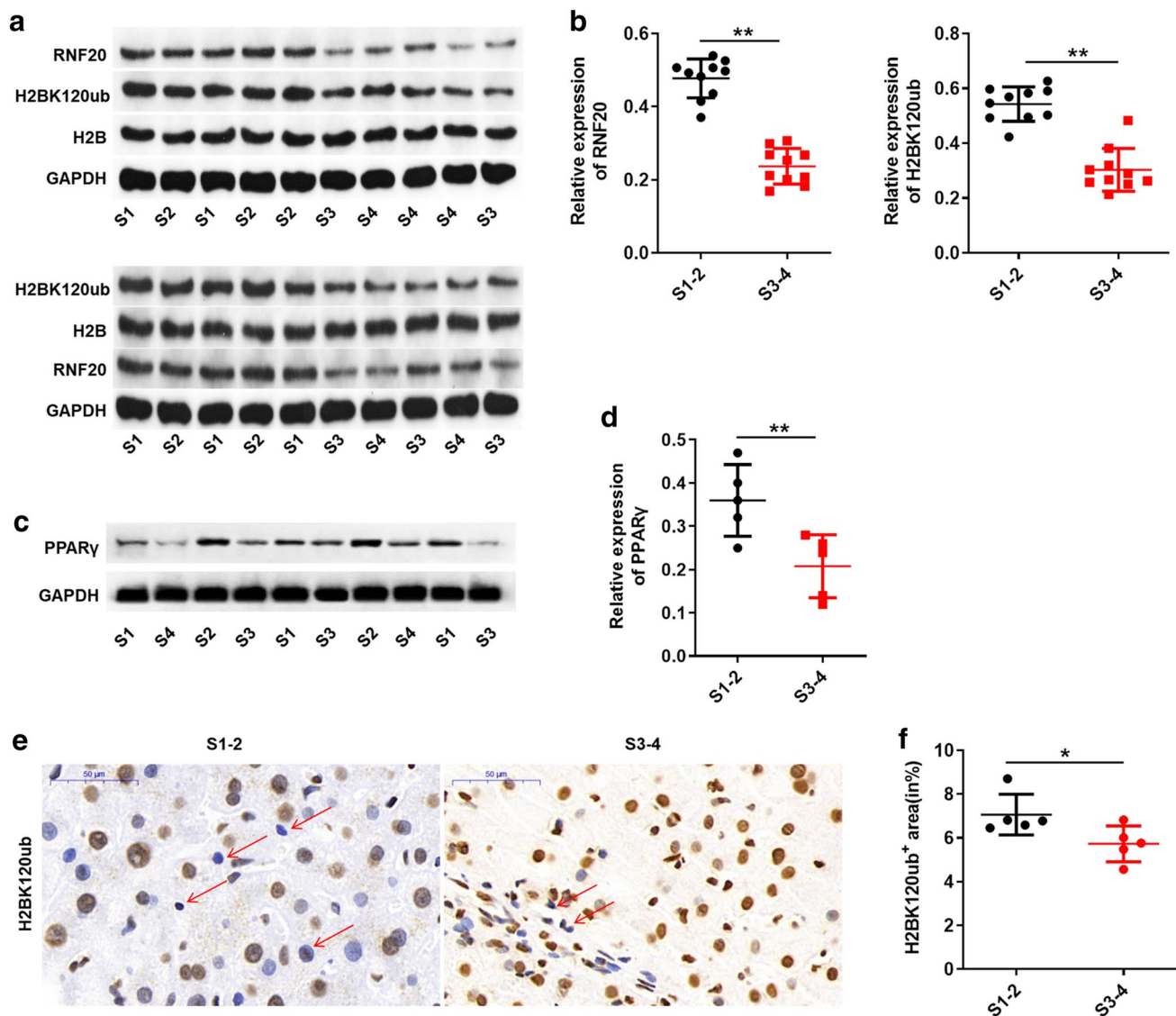


Fig. 1 RNF20 and H2BK120ub were downregulated in S4 phase liver fibrosis tissues. **a** The expressions of RNF20, H2B and H2BK120ub in liver tissues of patients were detected by western blot. **b** The relative expressions of RNF20 and H2BK120ub were quantified by normalizing to GAPDH and H2B, respectively. **c, d** The expression of PPAR γ in liver tissues of patients was detected by western blot.

The relative expression of PPAR γ was quantified by normalizing to GAPDH. **e** The expression of H2BK120ub in tissues of patients was detected by IHC staining. Red arrows indicate the positive hepatic stellate cells. **f** The percentage of H2BK120ub area was calculated. * $P < 0.05$, ** $P < 0.01$ compared to control

Table 2 The statistical analysis of age/sex correlation

	S1-S2 ($n=10$)	S3-S4 ($n=10$)	P value
Age (≥ 40 / < 40)	5/5	9/1	0.0510
Gender (male/female)	8/2	7/3	0.6056

VEGFA were closely correlated with the progression of liver fibrosis [19, 20]. Thus, these three cytokines were detected in following experiments.

Overexpression of RNF20 inhibited TGF- β -induced fibrosis in LX-2 cells via inactivation of IL-6, TNF- α and VEGFA

To investigate the mechanism by which RNF20 mediates the fibrosis, RT-qPCR was used. As revealed in Fig. 6a–c, TGF- β -induced increase of IL-6, TNF- α and VEGFA in LX-2 cells was significantly reversed by RNF20 overexpression. Therefore, overexpression of RNF20 inhibited TGF- β -induced fibrosis in LX-2 cells via inactivation of IL-6, TNF- α and VEGFA.

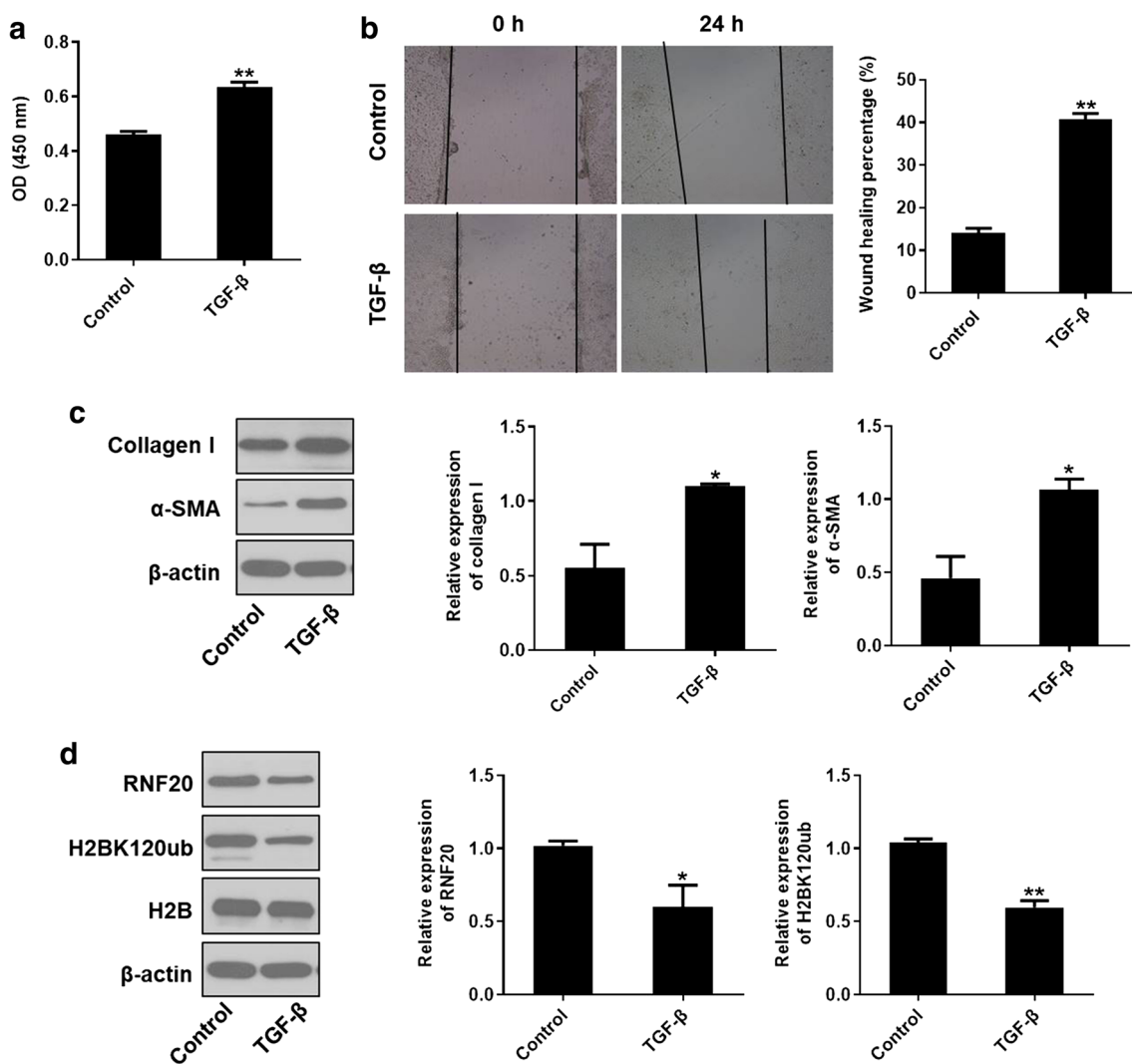


Fig. 2 In vitro model of liver fibrosis was successfully established. LX-2 cells were treated with 5 ng/ml TGF- β . Then, **a** the viability of LX-2 cells was measured by CCK-8 assay. **b** Cell migration was detected by wound healing assay. **c** The protein expressions of collagen I and α -SMA in LX-2 cells were detected by western blot. The

relative expressions were quantified by normalizing to GAPDH. **d** The protein expressions of RNF20, H2B and H2BK120ub in LX-2 cells were detected by western blot. The relative expressions of RNF20 and H2BK120UB were quantified by normalizing to GAPDH and H2B, respectively. * $P < 0.05$, ** $P < 0.01$ compared to control

RNF20 overexpression-induced inhibition of fibrosis was reversed by pcDNA3.1-H2BK120R

To further confirm the correlation between RNF20 and H2BK120ub, LX-2 cells were overexpressed with H2BK120R (H2B ubiquitination blocker), and then CCK8 assay was performed. As shown in Fig. 7a, TGF- β -induced increase of cell viability was significantly inhibited by RNF20 overexpression, while the effect of RNF20 overexpression was partially reversed by H2BK120R overexpression. Moreover, overexpression of H2BK120R partially reversed AAVRNF20-induced inactivation of VEGFA, IL-6 and TNF- α in TGF- β -treated LX-2 cells

(Fig. 7b–d). Consistently, overexpression of RNF20 significantly inhibited TGF- β -induced upregulation of collagen I and α -SMA, while this phenomenon was reversed by H2BK120R (Fig. 7e). In contrast, TGF- β -induced inactivation of H2BK120ub, RNF20 and PPAR γ was reversed in the presence of AAV-RNF20, and the effect of RNF20 overexpression on H2BK120ub and PPAR γ was partially reversed by H2BK120R overexpression (Fig. 7e). Meanwhile, upregulation of H2BK120R had very limited effect on RNF20 expression (Fig. 7e). In summary, RNF20 overexpression-induced inhibition of fibrosis was reversed by H2BK120R overexpression.

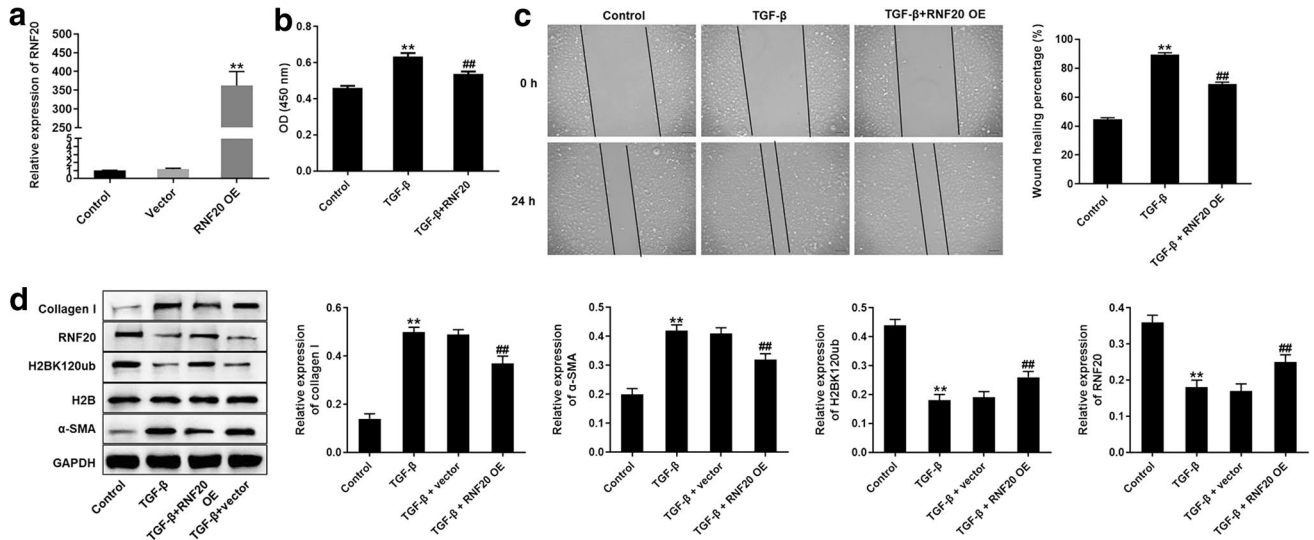


Fig. 3 Overexpression of RNF20 significantly inhibited TGF- β -induced fibrosis in LX-2 cells via mediation of H2BK120ub. **a** LX-2 cells were transfected with pcDNA3.1 or pcDNA3.1-RNF20. Then, efficiency of cell transfection was investigated by RT-qPCR. **b** The viability of LX-2 cells was measured by CCK-8 assay. **c** Cell migra-

tion was tested by wound healing assay. **d** The protein expressions of collagen I, α -SMA, RNF20 and H2BK120ub in LX-2 cells were detected by western blot. The relative expressions were quantified by normalizing to GAPDH or H2B. ** P < 0.01 compared to control. ## P < 0.01 compared to TGF- β

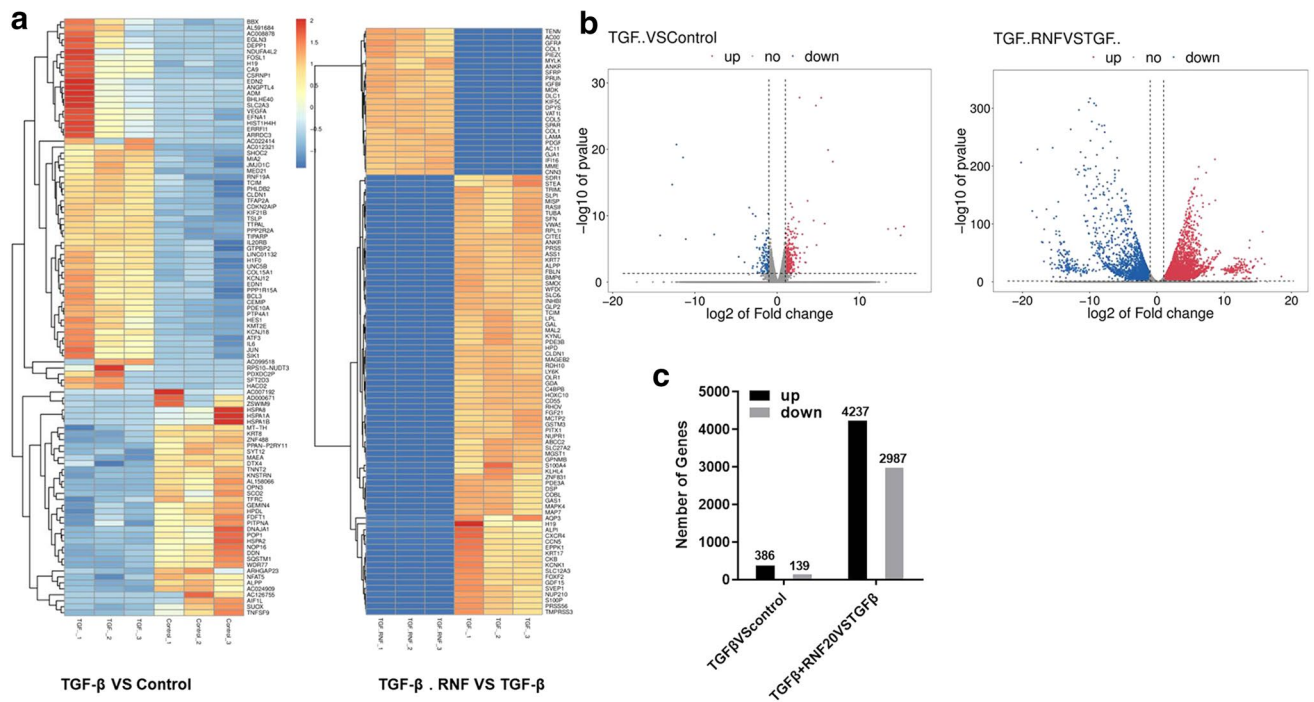


Fig. 4 Expression profiles of genes related with RNF20-mediated liver fibrosis. **a** The differentially expressed genes between control and TGF- β were presented by Volcano plot and heat map. **b** The differentially expressed genes between TGF- β and TGF- β plus RNF20

were presented by Volcano and heat map. **c** Number of differentially expressed genes between control and TGF- β , as well as TGF- β and TGF- β + RNF20 was calculated

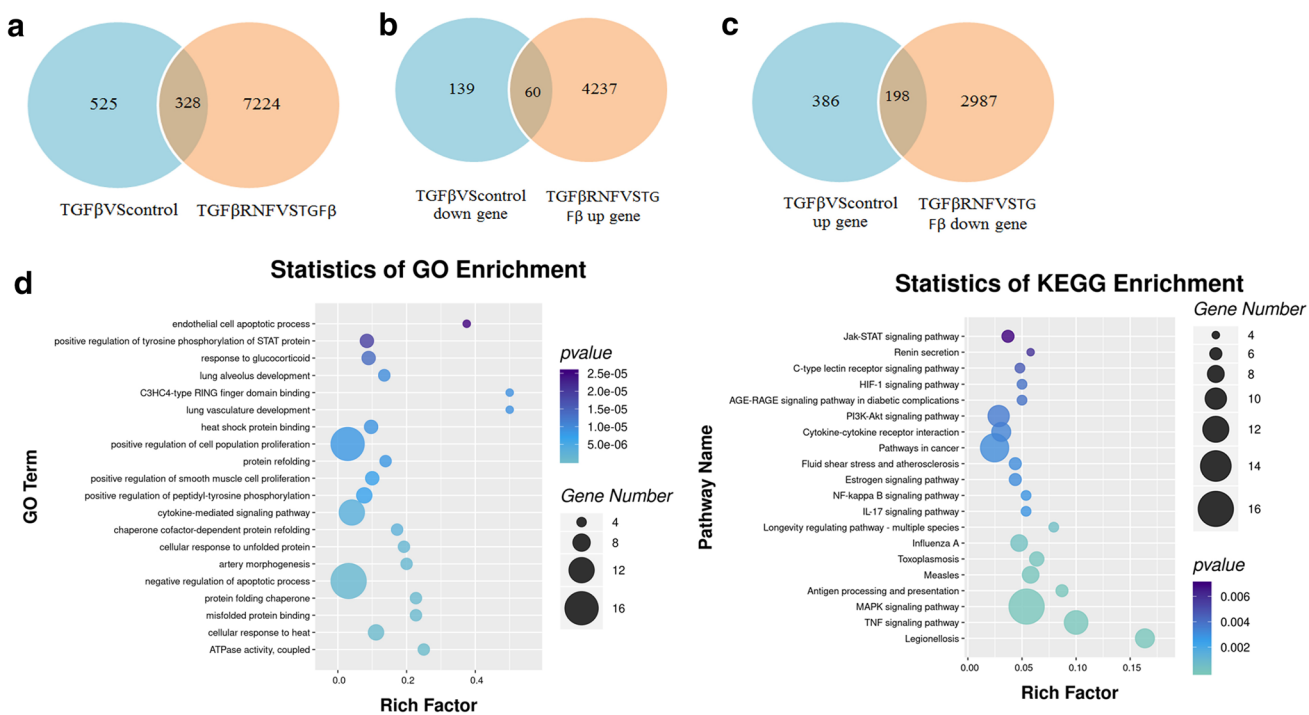


Fig. 5 The data of Go and KEGG analysis were presented. **a, b, c** Among 328 overlapped differentially expressed genes, 60 genes were down-regulated in TGF- β group and up-regulated in TGF- β +RNF20,

198 genes were up-regulated in TGF- β group and down-regulated in TGF- β +RNF20. **d** GO and KEGG analysis were performed to identify the genes associated with RNF20-mediated liver fibrosis

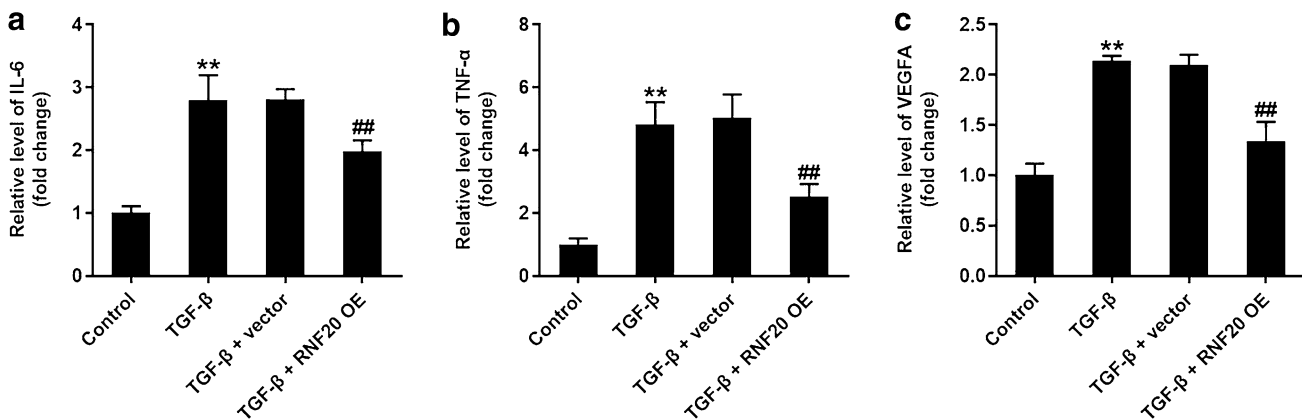


Fig. 6 Overexpression of RNF20 inhibited TGF- β -induced fibrosis in LX-2 cells via inactivation of IL-6, TNF- α and VEGFA. **a** The expression of IL-6 in LX-2 cells was detected by RT-qPCR. **b** The expression of TNF- α in LX-2 cells was detected by RT-qPCR. **c**

The expression of VEGFA in LX-2 cells was detected by RT-qPCR. ** $P < 0.01$ compared to control. # $P < 0.01$, ## $P < 0.01$ compared to TGF- β

Overexpression of RNF20 significantly alleviated the symptom of liver fibrosis in vivo

To investigate the function of RNF20 in liver fibrosis, in vivo model of liver fibrosis was established. As demonstrated in Fig. 8a, CCl4 significantly induced inflammatory infiltration in tissues of mice in a time-dependent

manner, while this phenomenon was reversed by overexpression of RNF20. In addition, CCl4-induced increase of collagen volume infarction was reversed by AAV-RNF20 (Fig. 8b). Meanwhile, the expression of α -SMA in tissues of mice was significantly increased by CCl4 (Fig. 8c). In contrast, CCl4 significantly decreased the expression of H2BK120ub in mice (Fig. 8d). Furthermore, the effect

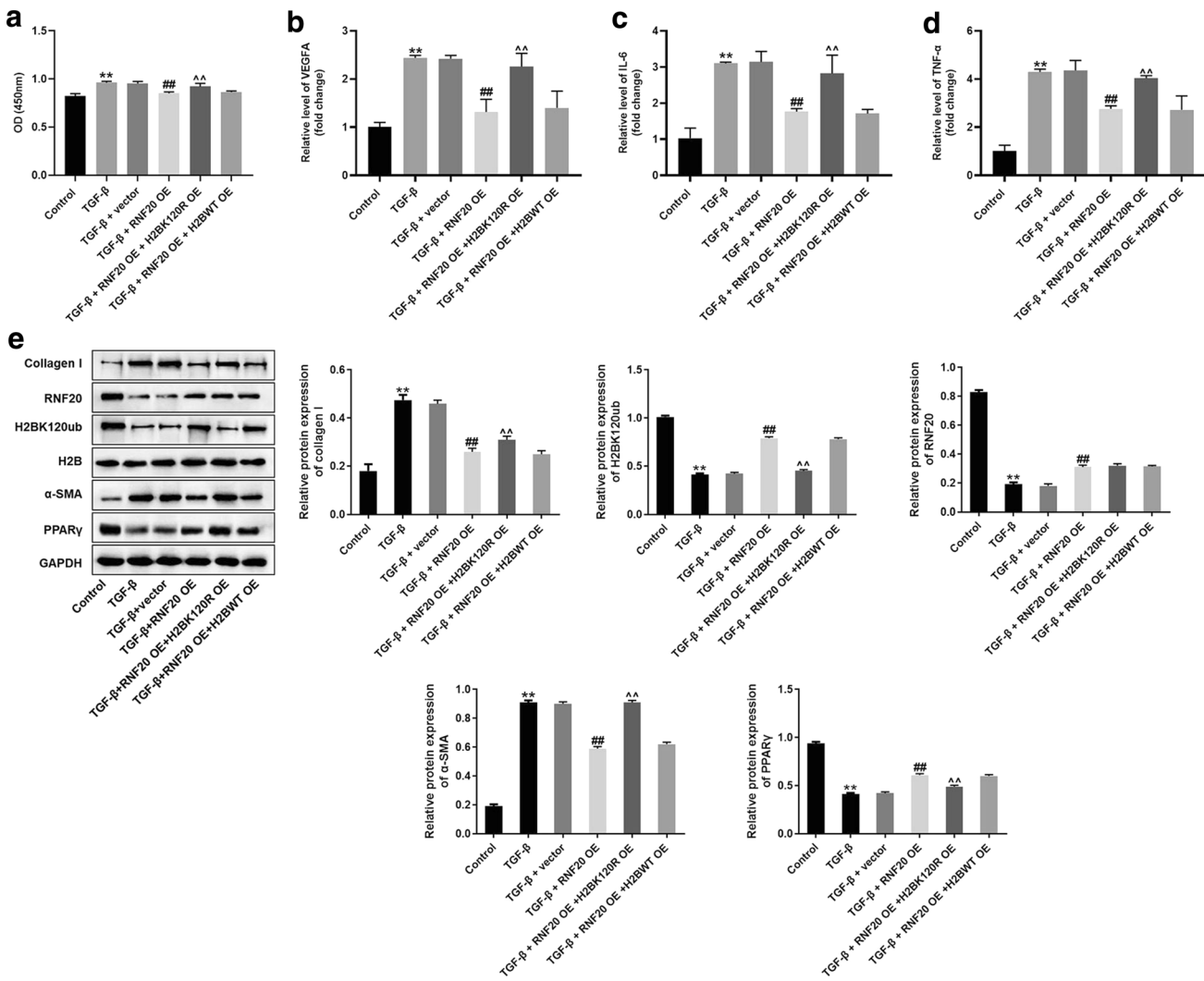


Fig. 7 RNF20 overexpression-induced inhibition of fibrosis was reversed by pcDNA3.1-H2BK120R. LX-2 cells were treated with TGF-β, TGF-β + vector, TGF-β + RNF20 OE, TGF-β + RNF20 OE + H2BK120R OE or TGF-β + RNF20 OE + H2BWT OE. **a** The viability of LX-2 cells was tested by CCK8 assay. **b-d** The levels of IL-6, VEGFA and TNF-α in LX-2 cells were detected by RT-qPCR. **e** The protein levels of H2BK120ub, H2B, collagen I, α-SMA,

RNF20 and PPAR γ in LX-2 cells were detected by western blot. The relative expressions of collagen I, α-SMA, RNF20 and PPAR γ were quantified by normalizing to GAPDH. The relative level of H2BK120ub was quantified by normalizing to H2B. **P < 0.01 compared to control. ##P < 0.01 compared to TGF-β. ^P < 0.01 compared to TGF-β + RNF20 OE

of CCl4 on these two proteins was significantly inhibited by overexpression of RNF20 (Fig. 8c and d). Taken together, overexpression of RNF20 significantly alleviated the symptom of liver fibrosis *in vivo*.

Overexpression of RNF20 attenuated the progression of liver fibrosis *in vivo* through mediation of H2BK120ub

Finally, to detect the protein expressions, western blot was performed. As revealed in Fig. 9a–c, CCl4-induced decrease of RNF20 and H2BK120ub in tissues of mice was reversed by overexpression of RNF20. In contrast, the expressions

of α-SMA and collagen I in mice were significantly upregulated by CCl4, while this phenomenon was reversed by RNF20 overexpression (Fig. 9a, d and e). Furthermore, CCl4-induced inactivation of PPAR γ in mice was reversed by RNF20 overexpression (Fig. 9f and g). Altogether, overexpression of RNF20 attenuated the progression of liver fibrosis *in vivo* through mediation of H2BK120ub.

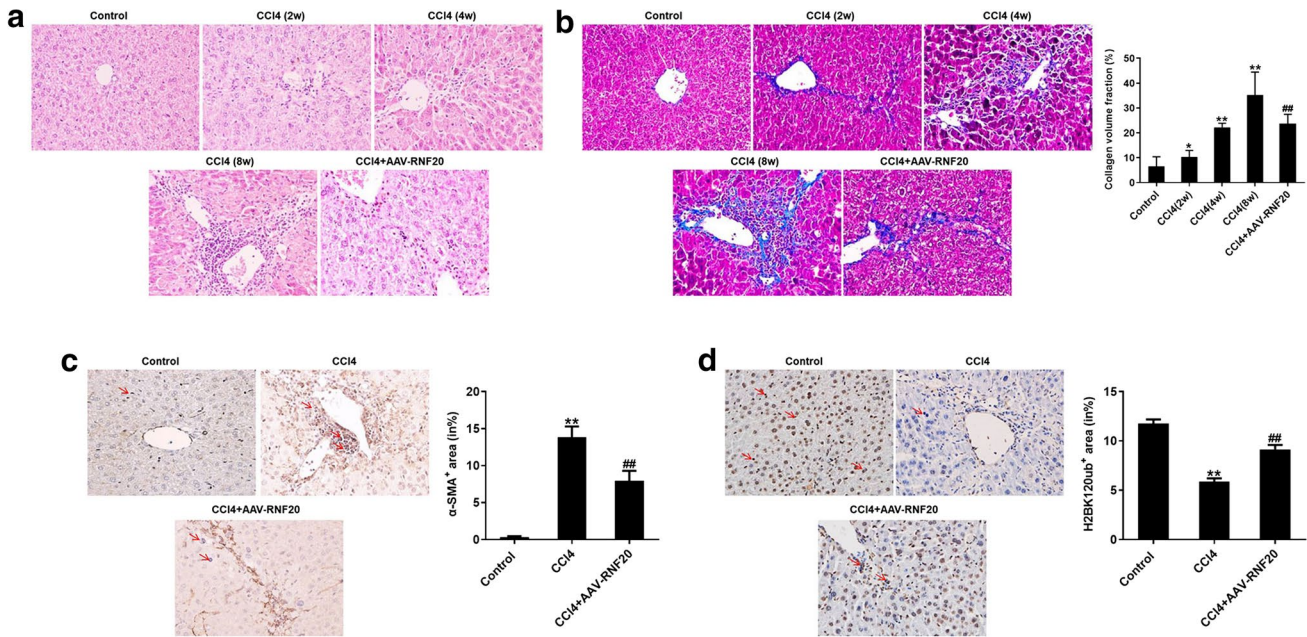


Fig. 8 Overexpression of RNF20 significantly alleviated the symptom of liver fibrosis in vivo. **a** The pathological analysis in liver tissues of mice was detected by HE staining. **b** The symptom of liver fibrosis was detected by Masson staining. The area of collagen volume frac-

tion was calculated. **c, d** The expressions of α -SMA and H2BK120ub in tissues of mice were detected by IHC staining. Red arrows indicate the positive hepatic stellate cells. ** $P < 0.01$ compared to control. ## $P < 0.01$ compared to CCl4

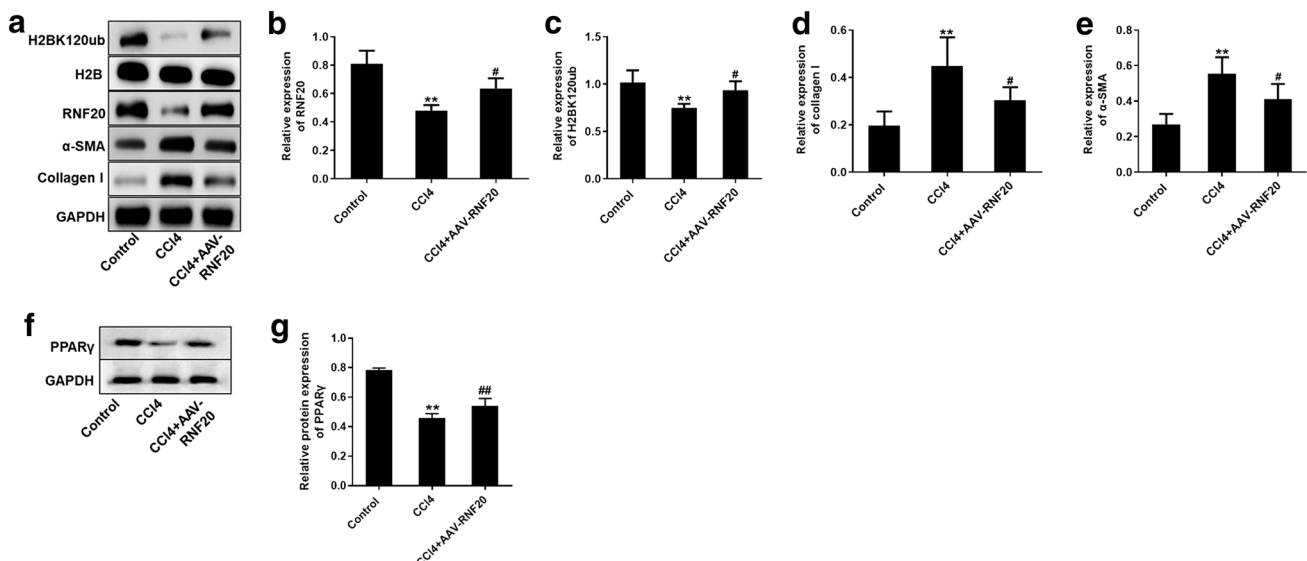


Fig. 9 Overexpression of RNF20 attenuated the progression of liver fibrosis in vivo through mediation of H2BK120ub. **a** The protein expressions of H2B, H2BK120ub, RNF20, α -SMA and collagen I in tissues of mice were detected by western blot. **b** The relative expression of RNF20 was quantified by normalizing to GAPDH. **c** The relative expression of H2B was quantified by normalizing to GAPDH. **d**

The relative expression of collagen I was quantified by normalizing to GAPDH. **e** The relative expression of α -SMA was quantified by normalizing to GAPDH. **f, g** The protein level of PPAR γ in tissues of mice was detected by western blot. The relative expression was quantified by normalizing to GAPDH. ** $P < 0.01$ compared to control. # $P < 0.01$ compared to CCl4

Discussion

In the current study, RNF20 inhibited the progression of liver fibrosis in vitro and in vivo via H2B ubiquitination. It has been proved that RNF20 could mediate the ubiquitination of H2B [5, 9]. Our data further confirmed the function of RNF20. In addition, this study firstly revealed the effect of RNF20 overexpression on progression of liver fibrosis, suggesting RNF20 may act as an inhibitor in liver fibrosis.

Mammalian RNF20/RNF40 complexes function similarly to their yeast homology Bre1 as ubiquitin ligases in monoubiquitination of Lys-120 of histone H2B [21]. Cells lacking RNF20 or expressing H2BK120R, which lead to a lack of ubiquitin conjugation sites, showed a dramatically reduced level of ubiquitylation [22]. Moreover, dysregulation of RNF20 upregulated or downregulated the level of H2Bub in humans [23] and mice [24]. In our study, the data revealed that the level of H2BK120ub is positively correlated RNF20. It suggested a key role for RNF20 and H2Bub in the regulation of liver tissue repairs.

Our finding revealed that TNF- α , IL-6 and VEGFA were key cytokines in RNF20-mediated liver fibrosis progression. TNF- α and IL-6 are two inflammatory mediators which are involved in liver fibrosis progression [19, 20]. VEGFA has been reported to be a key modulator in angiogenesis, which is known to mediate the development of liver fibrosis [25]. Our research was consistent to this previous research, firstly indicating the relation between RNF20 and these three cytokines in liver fibrosis. Meanwhile, RNF20 could inhibit the tumorigenesis via mediation of p53 [10]. P53 is a cell cycle-related protein which plays a crucial role in cancer cell growth [26], while IL-6 and TNF- α are inflammatory mediators. Therefore, different type of diseases may result in this difference.

RNF20 overexpression exhibited significantly anti-fibrotic effect via inactivation of α -SMA and collagenI. A previous research indicated that α -SMA is a key mediator in fibrosis [27]. Moreover, collagen I has been regarded to be upregulated during the progression of fibrosis [28]. Consistent to these previous researches, overexpression of RNF20 could attenuate the development of liver fibrosis via inhibition of α -SMA and collagen I in vitro and in vivo. Additionally, α -SMA played a key role in EMT process [29]. The data were similar to the recent report, suggesting that RNF20 overexpression may act as an EMT process inhibitor.

Frankly speaking, there are some limitations in this study. Firstly, the correlation between H2BK120ub and fibrotic proteins (α -SMA and collagen I) is unclear yet. In addition, a causal correlation between RNF20 and H2BK120ub in liver fibrosis needs to be further confirmed. Therefore, more investigations are needed in the future.

In conclusion, overexpression of RNF20 inhibited the progression of liver fibrosis via mediation of H2BK120ub. Thus, RNF20 might serve as a new target for the treatment of liver fibrosis.

Supplementary Information The online version contains supplementary material available at <https://doi.org/10.1007/s13577-021-00498-z>.

Author contributions HH design study and revised the manuscript; SC and XD analysis data and perform manuscript drafting; HL, YG and YZ search the literature and collect data; HH reviewed the results and made critical comments on the manuscript.

Funding The study was supported by the National Natural Science Foundation of China (No. 81672115).

Compliance with ethical standards

Conflict of interests These authors declared no competing interests in this research.

Ethical approval In vivo study, all the protocols were performed according to the guidelines of the Use Committee of Zhejiang Provincial People's Hospital (No. 20200004), and all the animal experiments were performed in accordance with National Institutes of Health guide for the care and use of laboratory animals. The clinical samples were collected in accordance with the Institutional Ethical Committee of Zhejiang Provincial People's Hospital.

References

1. Manning MW, Li YJ, Linder D, Haney JC, Wu YH, Podgoreanu MV, et al. (2020). Conventional Ultrafiltration During Elective Cardiac Surgery and Postoperative Acute Kidney Injury. *J Cardiothorac Vasc Anesth* S1053-0770:31271-4.
2. Gheorghe G, Bungau S, Ceobanu G, Ilie M, Bacalbasa N, Bratu OG, et al. The non-invasive assessment of hepatic fibrosis. *J Formos Med Assoc*. 2020;120:794–803.
3. Hukkanen M, Pihlajoki M, Pakarinen MP. Predicting native liver injury and survival in biliary atresia. *Semin Pediatr Surg*. 2020;29:150943.
4. Mellinger J, Winder GS, Fernandez AC (2020). HEP-20–1087: Measuring the Alcohol in Alcohol-related Liver Disease: Choices and Challenges for Clinical Research. *Hepatology* (Online ahead of print).
5. Liang X, Tao C, Pan J, Zhang L, Liu L, Zhao Y, et al. (2020). Rnf20 deficiency in adipocyte impairs adipose tissue development and thermogenesis. *Protein Cell* (Online ahead of print).
6. Zhao Y, Yang S, Wang Y, Tao C. Molecular characterization, expression profiling, and SNP analysis of the porcine RNF20 gene. *Animals (Basel)*. 2020;10:888.
7. Manikoth Ayyathan D, Koganti P, Marcu-Malina V, Litmanovitch T, Trakhtenbrot L, Emanuelli A, et al. SMURF2 prevents detrimental changes to chromatin, protecting human dermal fibroblasts from chromosomal instability and tumorigenesis. *Oncogene*. 2020;39:3396–410.
8. Jeon YG, Lee JH, Ji Y, Sohn JH, Lee D, Kim DW, et al. RNF20 functions as a transcriptional coactivator for PPARgamma by promoting NCoR1 degradation in adipocytes. *Diabetes*. 2020;69:20–34.

9. Robson A, Makova SZ, Barish S, Zaidi S, Mehta S, Drozd J, et al. Histone H2B monoubiquitination regulates heart development via epigenetic control of cilia motility. *Proc Natl Acad Sci USA*. 2019;116:14049–54.
10. Wu C, Cui Y, Liu X, Zhang F, Lu LY, Yu X. The RNF20/40 complex regulates p53-dependent gene transcription and mRNA splicing. *J Mol Cell Biol*. 2020;12:113–24.
11. Hooda J, Novak M, Salomon MP, Matsuba C, Ramos RI, MacDuffie E, et al. Early loss of histone H2B monoubiquitylation alters chromatin accessibility and activates key immune pathways that facilitate progression of ovarian cancer. *Cancer Res*. 2019;79:760–72.
12. Oh S, Boo K, Kim J, Baek SA, Jeon Y, You J, et al. The chromatin-binding protein PHF6 functions as an E3 ubiquitin ligase of H2BK120 via H2BK12Ac recognition for activation of trophectodermal genes. *Nucleic Acids Res*. 2020;48:9037.
13. Valencia-Sánchez MI, De Ioannes P, Wang M, Vasilyev N, Chen R, Nudler E, et al. Structural basis of dot1l stimulation by histone H2B lysine 120 ubiquitination. *Mol Cell*. 2019;74(1010–9):e6.
14. Wojcik F, Dann GP, Beh LY, Debelouchina GT, Hofmann R, Muir TW. Functional crosstalk between histone H2B ubiquitylation and H2A modifications and variants. *Nat Commun*. 2018;9:1394.
15. Desmet VJ, Gerber M, Hoofnagle JH, Manns M, Scheuer PJ. Classification of chronic hepatitis: diagnosis, grading and staging. *Hepatology*. 1994;19:1513–20.
16. Jia B, Zhang S, Wu S, Zhu Q, Li W. MiR-770 promotes oral squamous cell carcinoma migration and invasion by regulating the Sirt7/Smad4 pathway. *IUBMB Life*. 2020;73:264.
17. Zhang L, Liu X, Liang J, Wu J, Tan D, Hu W. Lefty-1 inhibits renal epithelial-mesenchymal transition by antagonizing the TGF-beta/Smad signaling pathway. *J Mol Histol*. 2020;51:77–87.
18. Zhu H, Shan Y, Ge K, Lu J, Kong W, Jia C. Specific overexpression of mitofusin-2 in hepatic stellate cells ameliorates liver fibrosis in mice model. *Hum Gene Ther*. 2020;31:103–9.
19. ElInfarawy AA, Nashy AE, Abozaid AM, Komber IF, Elweshahy RH, Abdelrahman RS. Vinpocetine attenuates thioacetamide-induced liver fibrosis in rats. *Hum Exp Toxicol*. 2020;2020:960327120947453.
20. Sheng J, Zhang B, Chen Y, Yu F. Capsaicin attenuates liver fibrosis by targeting Notch signaling to inhibit TNF-alpha secretion from M1 macrophages. *Immunopharmacol Immunotoxicol*. 2020;42:1–10.
21. Xu Z, Song Z, Li G, Tu H, Liu W, Liu Y, et al. H2B ubiquitination regulates meiotic recombination by promoting chromatin relaxation. *Nucleic Acids Res*. 2016;44:9681–97.
22. Tarcic O, Pateras IS, Cooks T, Shema E, Kanterman J, Ashkenazi H, et al. RNF20 links histone H2B ubiquitylation with inflammation and inflammation-associated cancer. *Cell Rep*. 2016;14:1462–76.
23. Chernikova SB, Razorenova OV, Higgins JP, Siscic BJ, Nicolau M, Dorth JA, et al. Deficiency in mammalian histone H2B ubiquitin ligase Bre1 (Rnf20/Rnf40) leads to replication stress and chromosomal instability. *Cancer Res*. 2012;72:2111–9.
24. Vethantham V, Yang Y, Bowman C, Asp P, Lee JH, Skalnik DG, et al. Dynamic loss of H2B ubiquitylation without corresponding changes in H3K4 trimethylation during myogenic differentiation. *Mol Cell Biol*. 2012;32:1044–55.
25. de Oliveira A, Castanhole-Nunes MMU, Biselli-Chicote PM, Pavarino EC, da Silva R, da Silva RF, et al. Differential expression of angiogenesis-related miRNAs and VEGFA in cirrhosis and hepatocellular carcinoma. *Arch Med Sci*. 2020;16:1150–7.
26. Lee KT, Islam F, Vider J, Martin J, Chruscik A, Lu CT, et al. Overexpression of family with sequence similarity 134, member B (FAM134B) in colon cancers and its tumor suppressive properties in vitro. *Cancer Biol Ther*. 2020;21:1–9.
27. Gong H, Fan Z, Yi D, Chen J, Li Z, Guo R, et al. Histidine kinase NME1 and NME2 are involved in TGF-beta1-induced HSC activation and CCl4-induced liver fibrosis. *J Mol Histol*. 2020;51:573.
28. Xue Y, Fan X, Yang R, Jiao Y, Li Y. miR-29b-3p inhibits post-infarct cardiac fibrosis by targeting FOS. *Biosci Rep*. 2020;40:BSR20201227.
29. Song XH, Chen XZ, Chen XL, Liu K, Zhang WH, Mo XM, et al. Peritoneal metastatic cancer stem cells of gastric cancer with partial mesenchymal-epithelial transition and enhanced invasiveness in an intraperitoneal transplantation model. *Gastroenterol Res Pract*. 2020;2020:3256538.

Publisher's Note Springer Nature remains neutral with regard to jurisdictional claims in published maps and institutional affiliations.